Advanced classification of VHR and SAR images

Fabio Del Frate, *University of Rome "Tor Vergata"*

Fully automatic classification of urban areas with high resolution SAR imagery (ERS/ENVISAT)

Geoinformation

Tor Vergata

Training Data Set

Site Information		Images Information			
Location	Dimension (km^2)	Acquisition Date	Satellite	B_p (m)	Dimension (pixels)
Rome, Italy	836	January 25, 1994	ERS 1	89	1245 x 1300
		January 31, 1994	ERS 1		
		March 26, 1994	ERS 1	157	
		March 29, 1994	ERS 1		
		July 13, 1994	ERS 1	-	
		February 13, 1999	ERS 1	211	
		February 14, 1999	ERS 2		
		March 20, 1999	ERS 1	65	
		March 21, 1999	ERS 2		
		July 4, 1999	ERS 2	-	

Test Data Set

Site Information		Images Information			
Location	Dimension (km^2)	Acquisition Date	Satellite	B_p (m)	Dimension (pixels)
Rome, Italy	836	February 24, 1996	ERS 1	12	1245 x 1300
		February 25, 1996	ERS 2		
		March 30, 1996	ERS 1	106	
		March 31, 1996	ERS 2		
		July 14, 1996	ERS 2	-	

Input Features

Careful selection and suitable processing are required to exploit the various pieces of information embedded in the amplitude, its time-space behavior and phase of the radar return:

- backscattering → mean intensity / intensity st. deviation
- interferometric coherence → late winter / early summer coherence
- textural features → Gray-Level Co-occurence Matrix (GLCM)

↓

Contrast – Energy (literature review)

↓

Window size : 7x7, 11x11 and 15x15

Input Features

Mean Int.

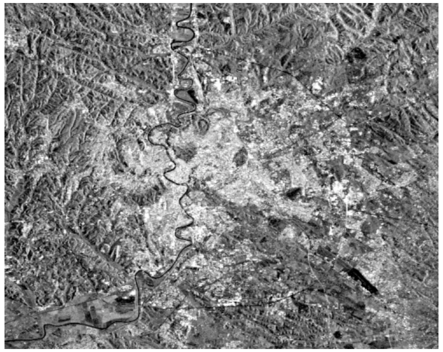

Int. St. Dev.

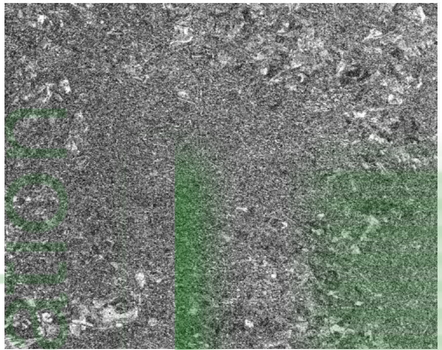

Wint. Coh.

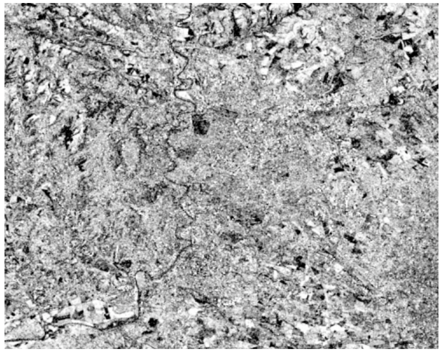

Spr. Coh.

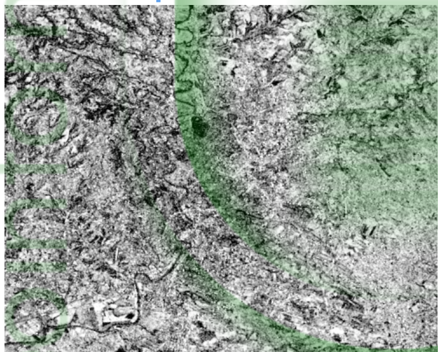

Contrast

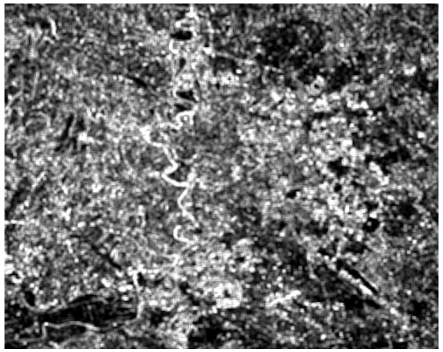

Energy

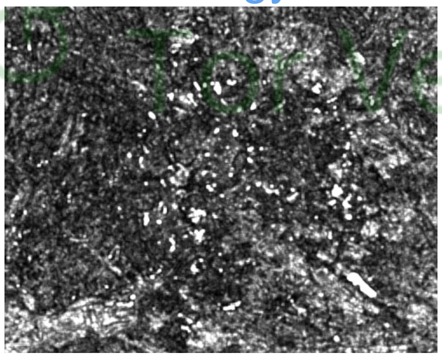

Long-term	
1	Mean Int.
2	Int. St. Dev.
3	Wint. Coh.
4	Spr. Coh.
5	Contrast
6	Energy

5 images

Short-term	
1	Mean Int.
2	Spr. Coh.
3	Contrast
4	Energy

2 images

Class Definition

These sets of 6 and 4 parameters respectively are exploited to discriminate among seven urban/sub-urban classes, including water surfaces (WS), vegetation (VE), forest (FO), asphalted surfaces (AS), isolated large buildings (IB) and continuous high/low density residential areas (HD/LD)

Classes	TR	VS
Asphalt (AS)	511	219
Forest (FO)	2592	1326
High Density (HD)	648	278
Isolated Buildings (IB)	122	433
Low Density (LD)	4900	6130
Vegetation (VE)	3535	6008
Water (WS)	892	382
Total	**13200**	**14776**

Neural Network Approach

The pieces of information extracted from the SAR images are fused and processed by a supervised Multi-Layer Perceptron (MLP) neural network which is known to show a considerable ease in using multi-domain data sources

We recorded the classification accuracies yielded by a varying number of hidden neurons, starting from a small topology (6-12-12-7) to end with a large one (6-100-100-7). The variance of the accuracy for different initializations of the weights was computed to monitor the stability of the algorithm

The Magnitude Based Pruning procedure has then been applied to thin the net

Short-term automatic mode - 4 inputs 1996

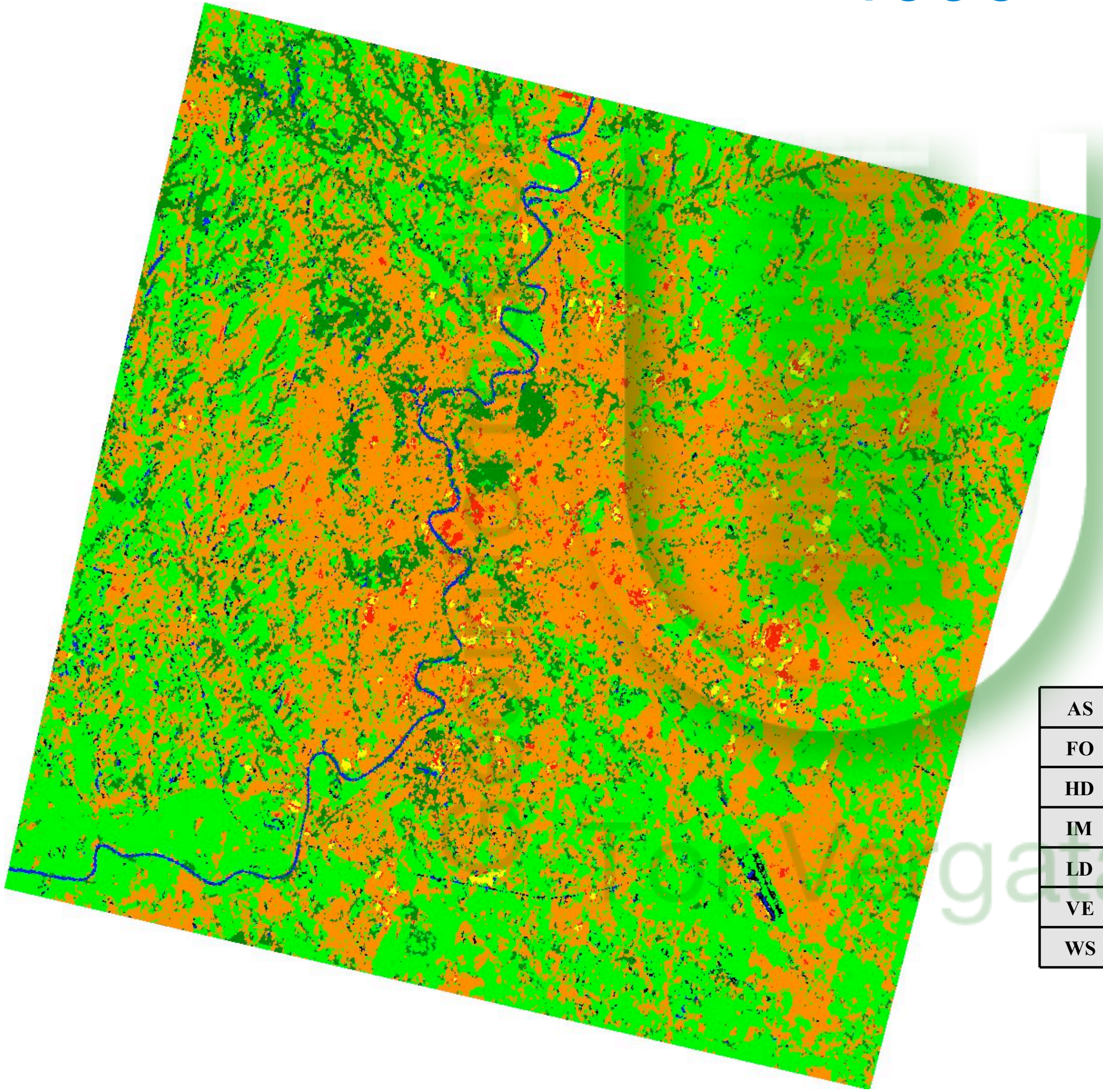

Classes	
Asphalt (AS)	
Forest (FO)	
High Density (HD)	
Isolated Buildings (IB)	
Low Density (LD)	
Vegetation (VE)	
Water (WS)	

	AS	FO	HD	IM	LD	VE	WS
AS	46.15	1.65	0.00	0.00	1.10	43.41	7.69
FO	1.90	69.16	0.00	0.00	15.22	10.60	3.13
HD	0.00	0.47	26.42	0.00	72.64	0.47	0.00
IM	0.00	0.00	4.91	78.13	13.84	3.13	0.00
LD	0.05	2.79	0.39	0.00	91.34	5.39	0.03
VE	1.29	2.55	0.00	0.00	8.08	87.94	0.13
WS	1.22	3.95	0.00	0.00	0.00	3.95	88.15
	Overall Er.(%)		13.52		k-Coefficient		0.780

Long-term automatic mode - 6 inputs 1996

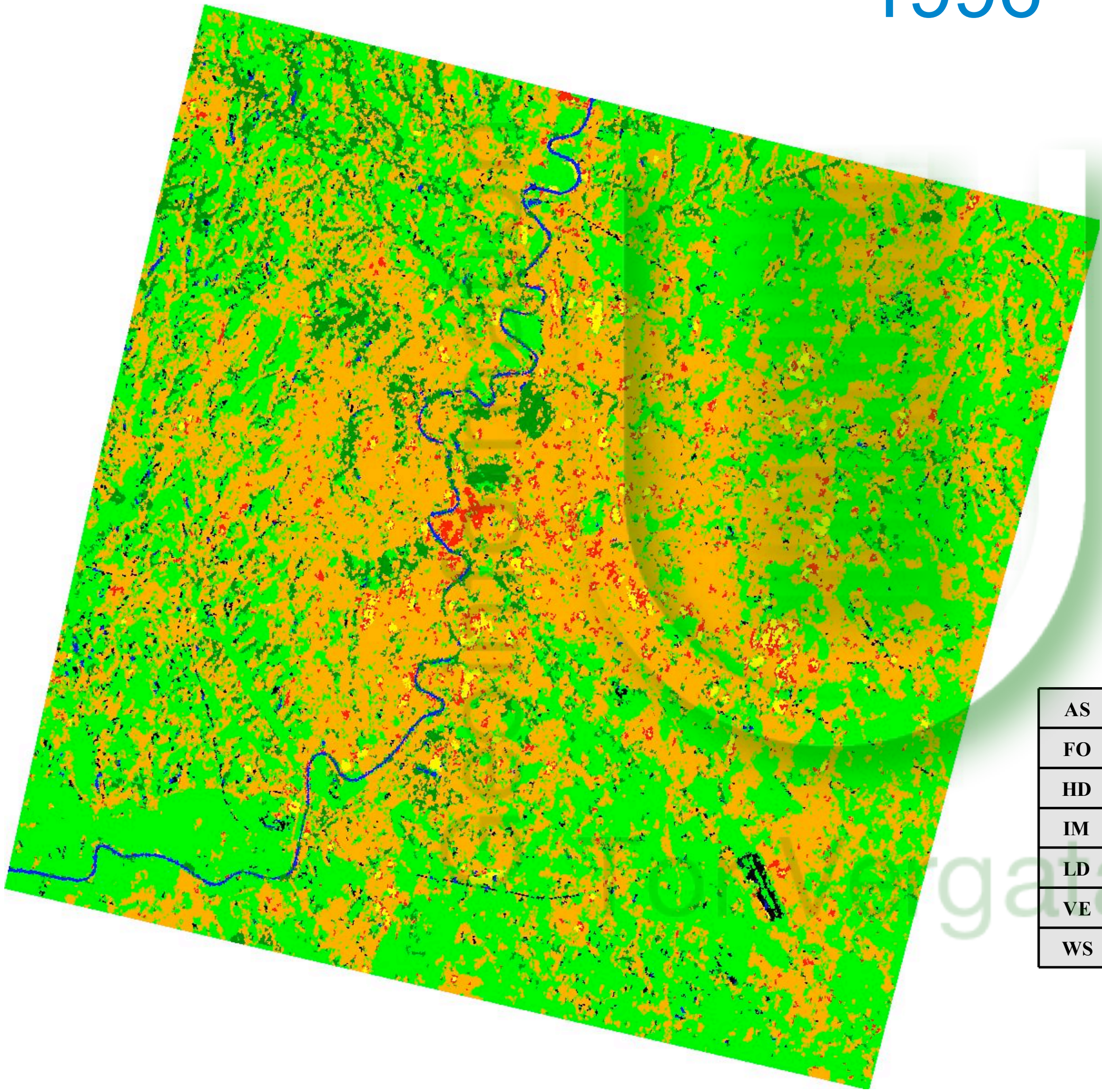

Classes	
Asphalt (AS)	
Forest (FO)	
High Density (HD)	
Isolated Buildings (IB)	
Low Density (LD)	
Vegetation (VE)	
Water (WS)	

	AS	FO	HD	IM	LD	VE	WS
AS	47.80	0.55	0.00	0.55	5.49	42.86	2.75
FO	0.41	71.74	0.00	0.00	15.22	11.14	1.49
HD	0.00	0.00	43.40	0.00	56.13	0.47	0.00
IM	0.00	0.00	16.52	79.46	3.13	0.89	0.00
LD	0.02	0.64	5.92	0.67	89.28	3.48	0.00
VE	1.35	1.44	0.21	0.01	4.71	92.23	0.04
WS	0.91	6.69	0.00	0.00	0.91	2.43	86.32
	Overall Er.(%)		11.73		k-Coefficient		0.811

Long-term automatic mode - 6 inputs 1996

The origin of most of the errors relies in the misclassification of HD as LW, which, given the contiguity of the two classes, can be recognized as a minor drawback.

If we merge these two classes, the overall accuracy reaches 91.5% (*K*-Coeff.=0.860) which can represent a satisfactory target for this type of application.

Classes	
Asphalt (AS)	
Forest (FO)	
High Density (HD)	
Isolated Buildings (IB)	
Low Density (LD)	
Vegetation (VE)	
Water (WS)	

	AS	FO	HD	IM	LD	VE	WS
AS	47.80	0.55	0.0[illegible]	0.55	5.49	42.86	2.75
FO	0.41	71.7[illegible]	0.00	0.0[illegible]	15.22	11.14	1.49
HD	0.00	0.00	43.40	0.00	56.13	0.47	0.00
IM	0.00	0.00	16.52	79.46	3.13	0.89	0.00
LD	0.02	0.64	5.92	0.67	89.28	3.48	0.00
VE	1.35	1.44	0.21	0.01	4.71	92.23	0.04
WS	0.91	6.69	0.00	0.00	0.91	2.43	86.32
	Overall Er.(%)		11.73		k-Coefficient		0.811

Classification detail

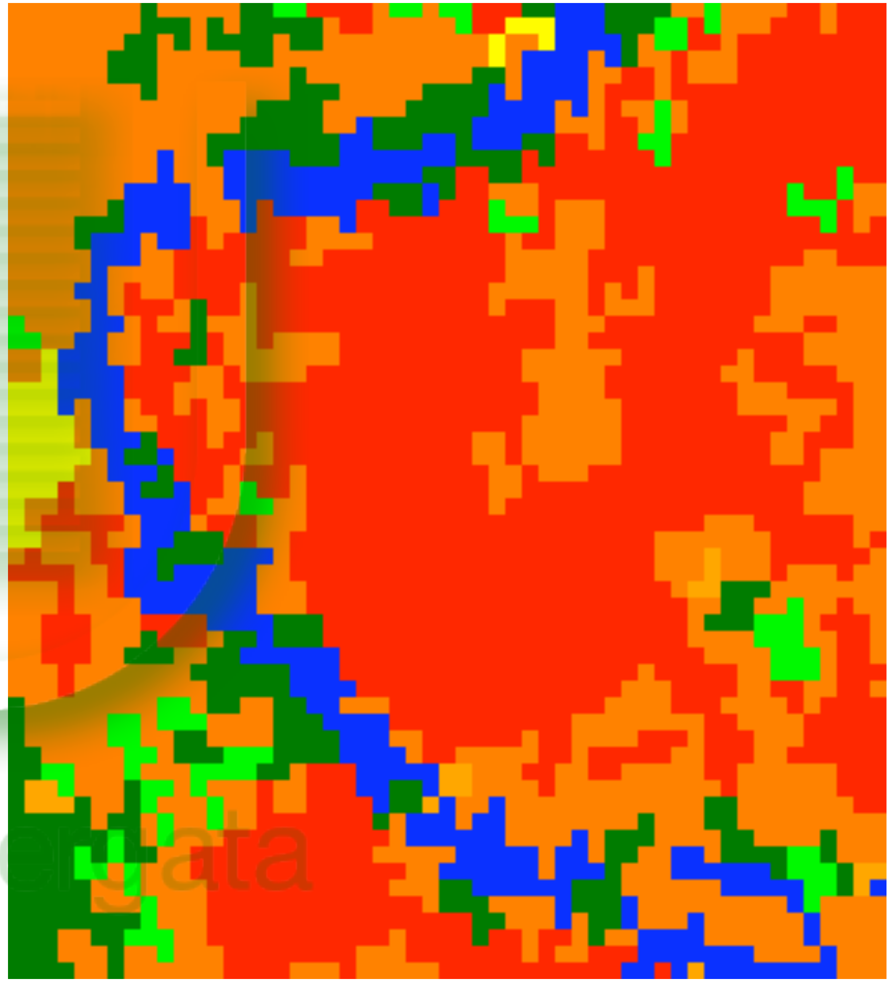

Change Detection 1994-1999

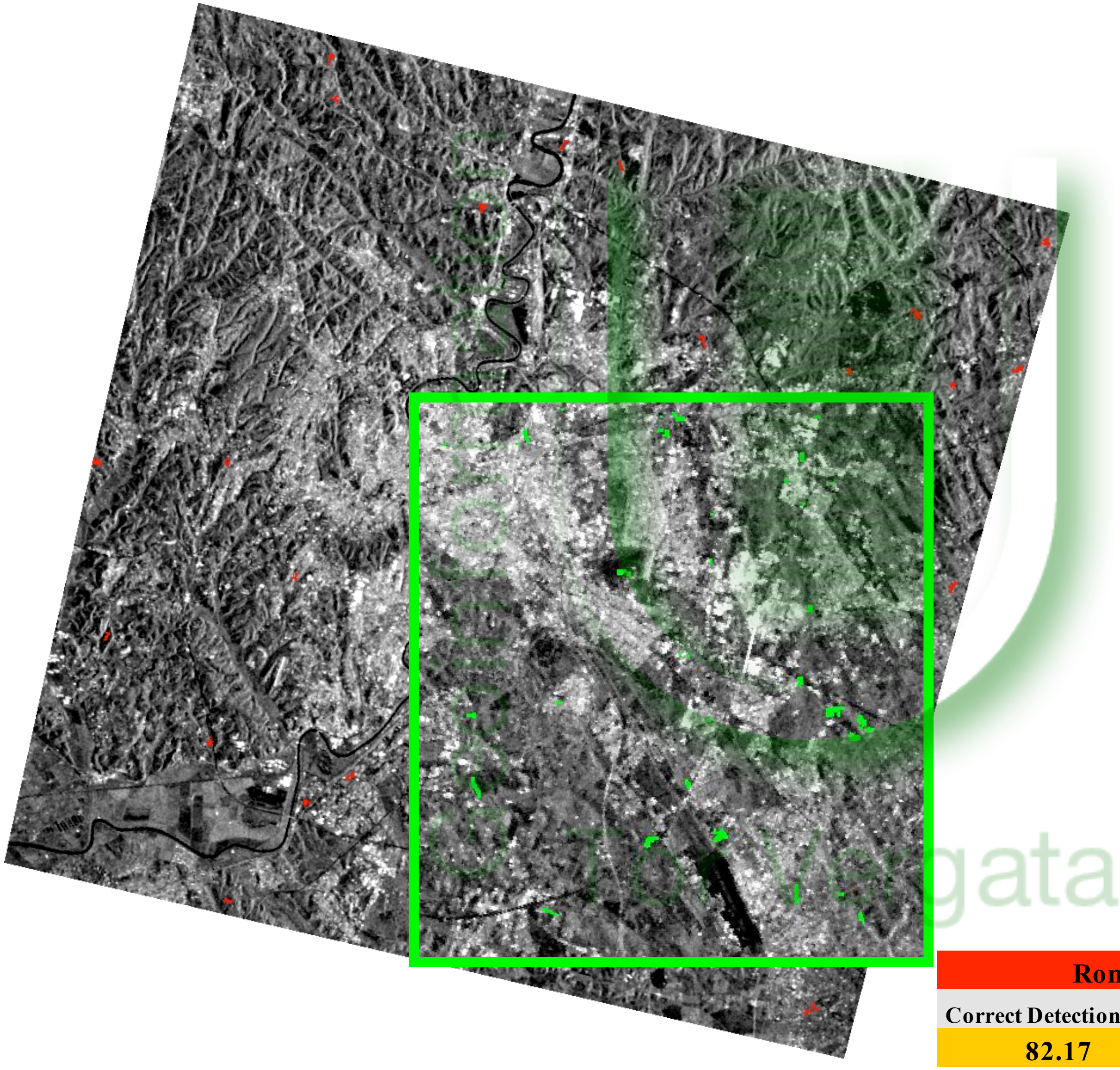

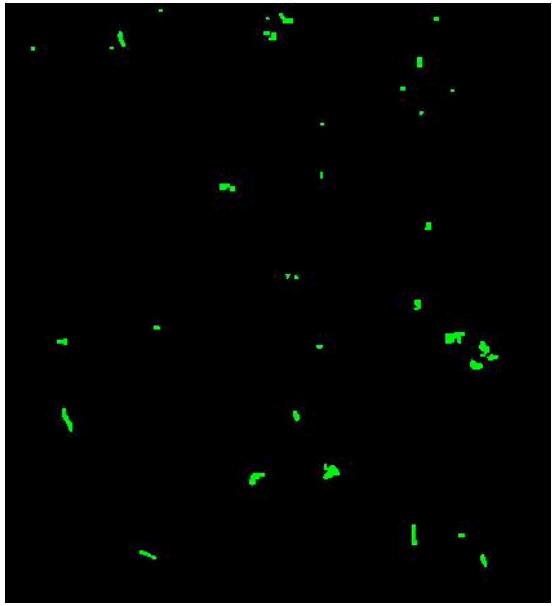

Rome SE: 160km² - 423x465pixels		
Correct Detection (%)	False Alarms (%)	Missed Alarms (%)
82.17	17.83	0.26

Pulse Coupled Neural Networks (PCNN) for Change detection with Very High Resolution imagery

Pulse-coupled neural network (PCNN)

The pulse-coupled neural network (PCNN) is a relatively new technique based on the implementation of the mechanisms underlying the visual cortex of small mammals.

PCNN is an algorithm that produces a series of binary pulse images when stimulated with a gray scale or color input.

It is different from what we generally mean with artificial neural networks in the sense that it does not need to be trained.

The Neuron Model (1/2)

The network consists of multiple nodes coupled together with their neighbors within a definite radius, forming a grid (2Dvector)

The PCNN neuron has two input compartments: linking and feeding. The feeding compartment receives both an external and a local stimulus, whereas the linking compartment only receives a local stimulus

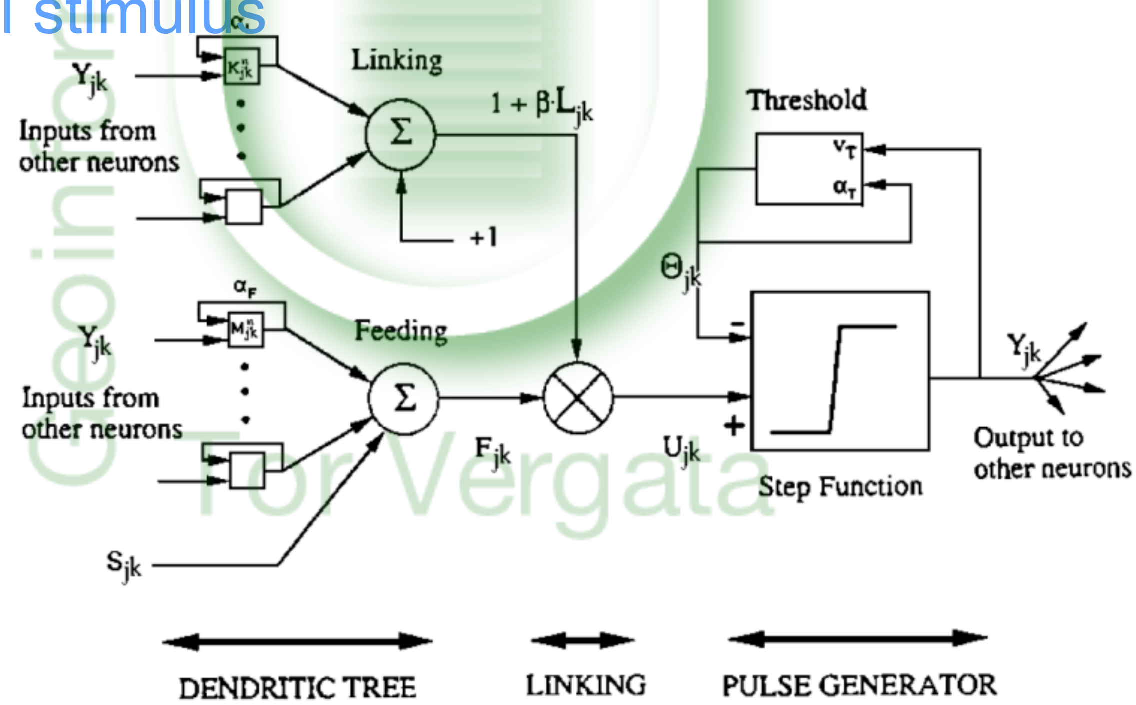

The Neuron Model (2/2)

The internal activity rises until it becomes larger than an active threshold value. Then the neuron fires and the threshold will decay until once again the internal activity becomes larger. Such a process gives rise to the pulsing nature of the PCNN

$$F_{ij}[n] = e^{\alpha_F \delta_n} F_{ij}[n-1] + S_{ij} + V_F \sum_{kl} M_{ijkl} Y_{kl}[n-1]$$

$$L_{ij}[n] = e^{\alpha_F \delta_n} L_{ij}[n-1] + V_L \sum_{kl} W_{ijkl} Y_{kl}[n-1]$$

$$U_{ij}[n] = F_{ij}[n]\{1 + \beta L_{ij}[n]\}$$

$$Y_{ij}[n] = \begin{cases} 1 \ if \ U_{ij}[n] > \Theta_{ij}[n-1] \\ 0 \quad Otherwise \end{cases}$$

$$\Theta_{ij}[n] = e^{\alpha_\Theta \delta_n} \Theta_{ij}[n-1] + V_\Theta Y_{ij}[n]$$

$$G[n] = \sum_{i,j} Y_{ij}[n]$$

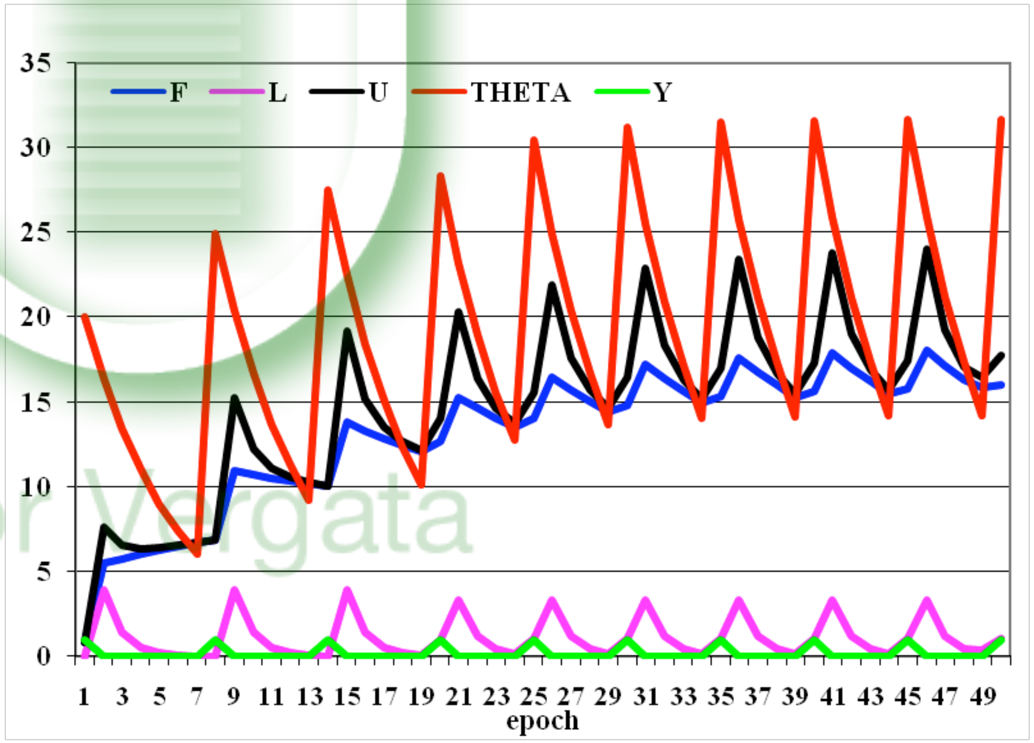

Change Detection

The waves generated in a moving window by each iteration of the algorithm create specific signatures of the scene which are successively compared for the change detection

We considered very-high resolution imagery. False alarms due to different geometrical views (misregistration or different acquisition angle) are typical for this kind of data

SIGNATURE ANALYSIS – The signal associated to the PCNN is invariant to changes in rotation, scale, shift, or skew of an object within the scene. These features make PCNN a promising tool for sub-metric change detection applications

Correlation Analysis

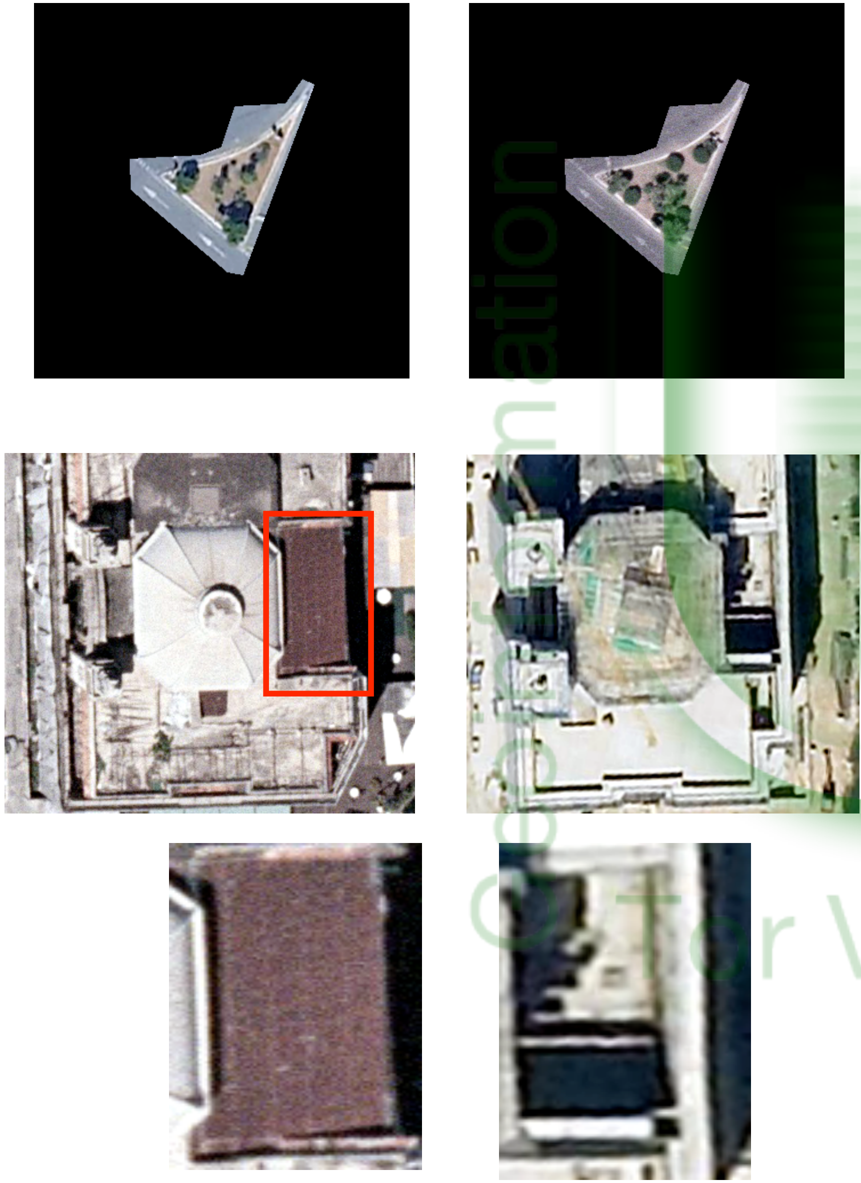

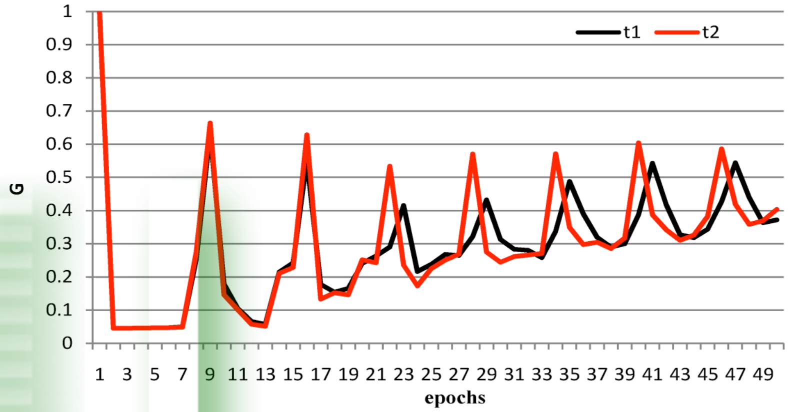

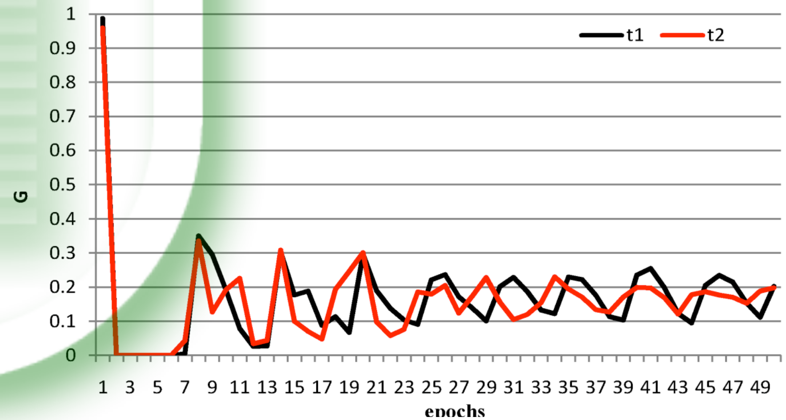

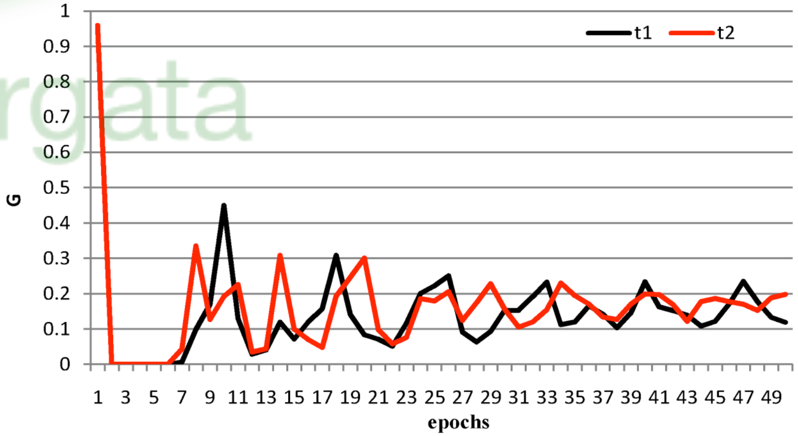

Example of results

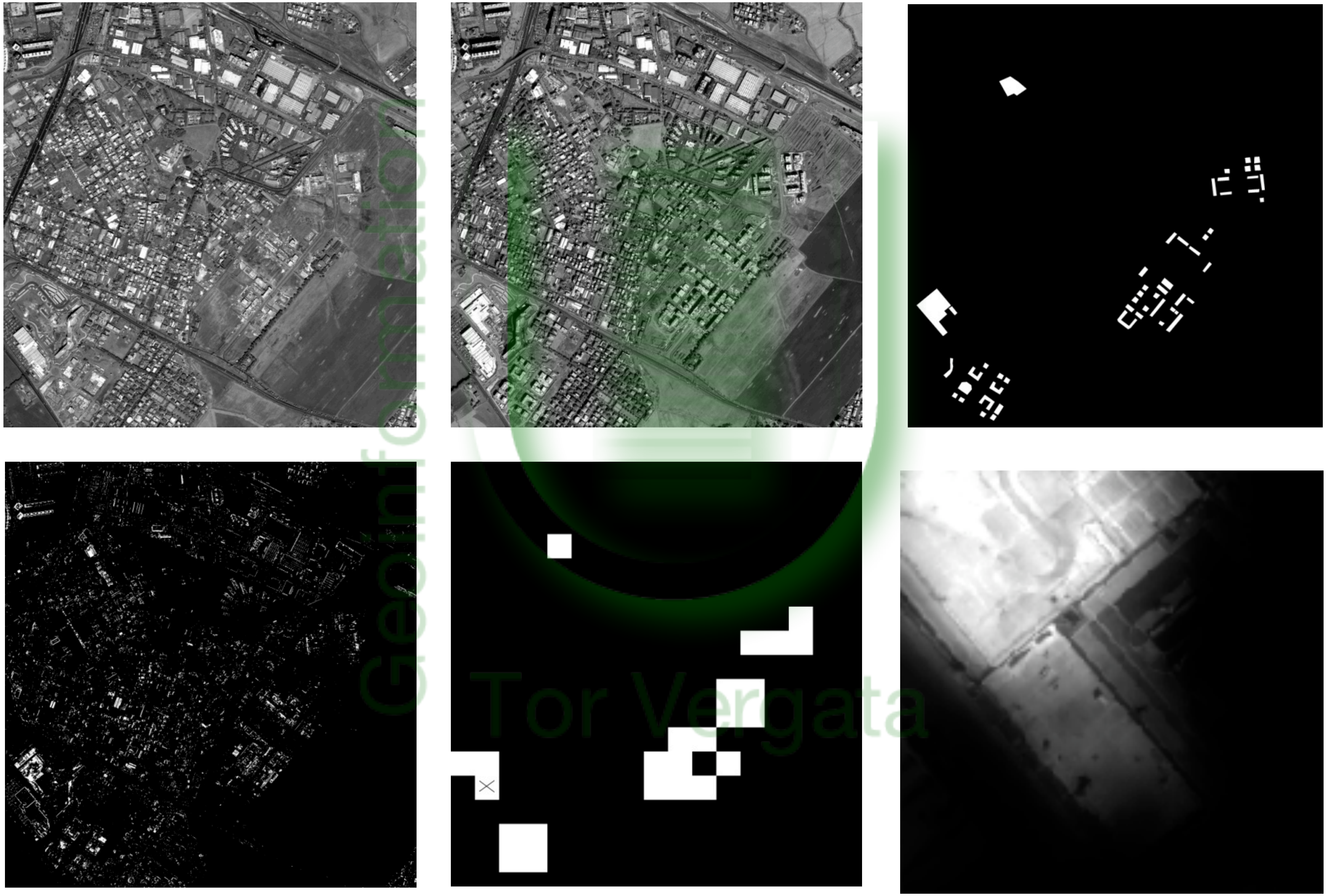

Towards Fully Automatic Scheme

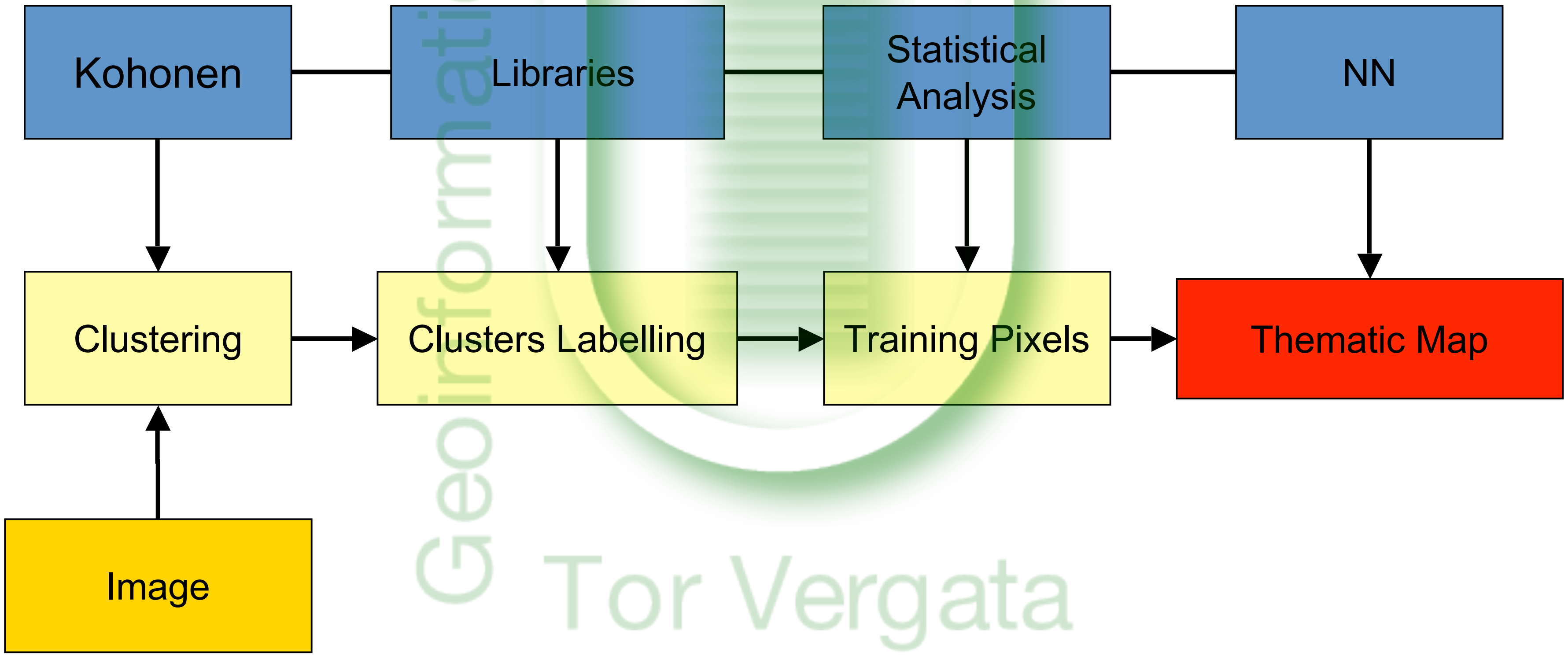

Polarimetric SAR imagery

L- band polarimetric NASA-JPL AirSAR - Montespertoli (FI) t

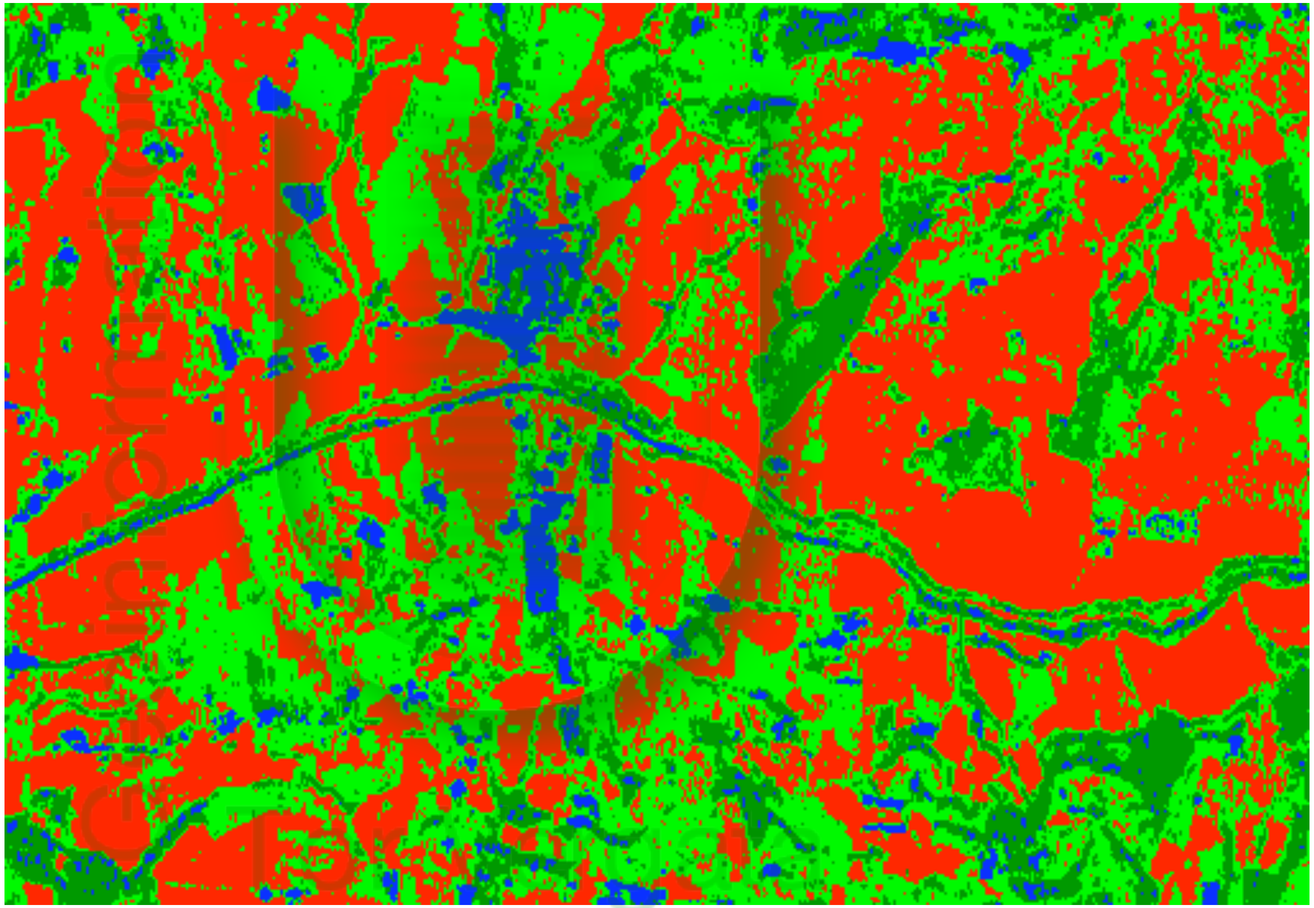

Blu : Urban
Dark green: woodland
Green:
Oliveyard,vineyards,colza
Red: sunflower and other

Overall Accuracy 82%

Very High Resolution Multispectral Imagery

Quickbird - Tor Vergata, Rome, test site

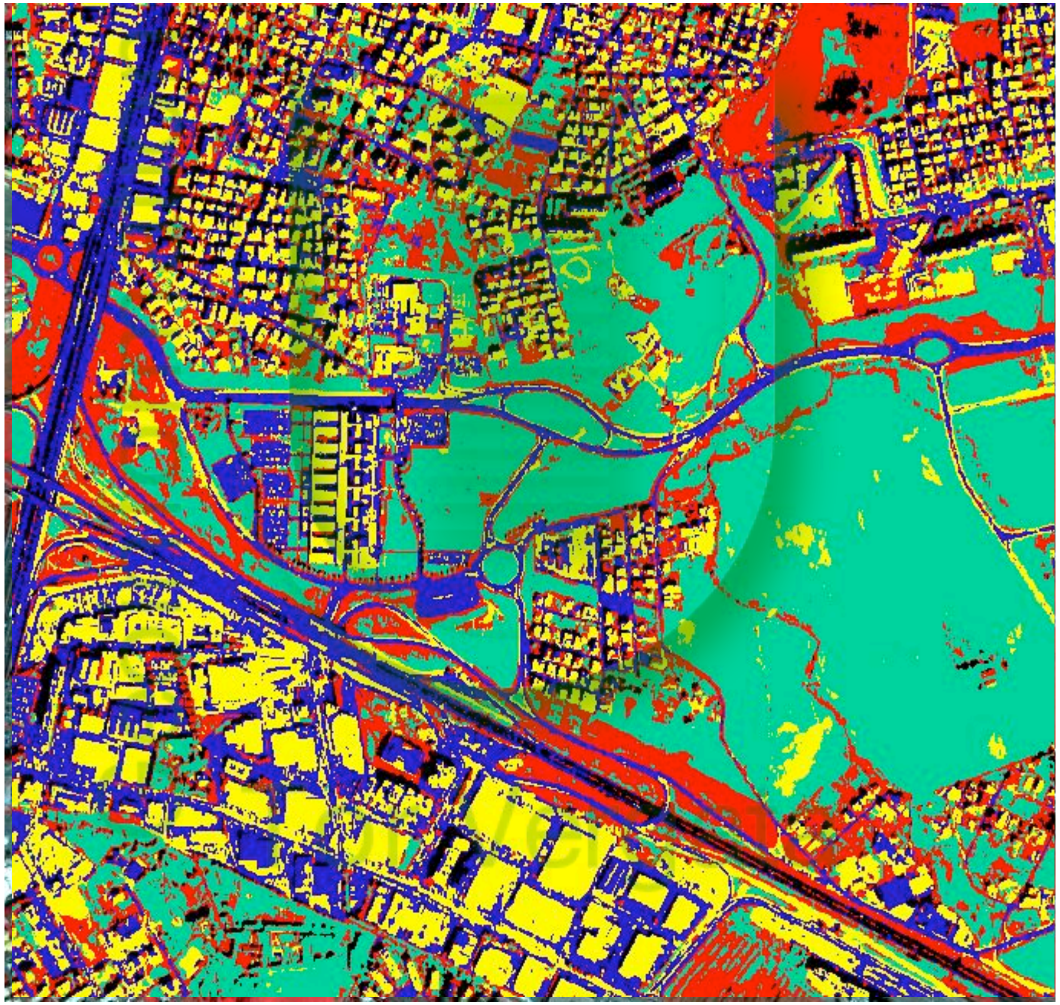

Overall Accuracy = 93.44%

TERRASAR-X IMAGING FOR UNSUPERVISED FIRE MAPPING

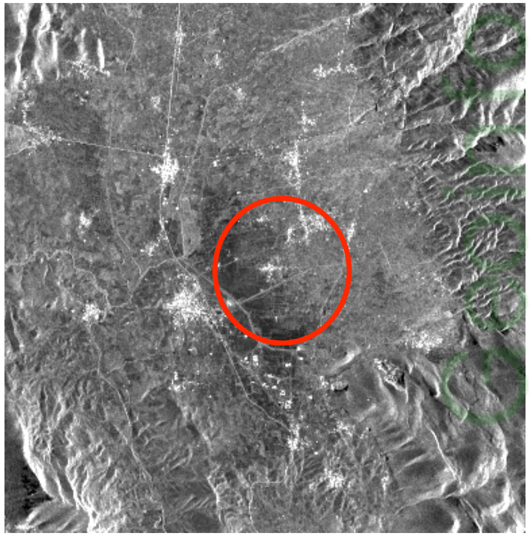

TerraSAR-X, HH

Landsat TM

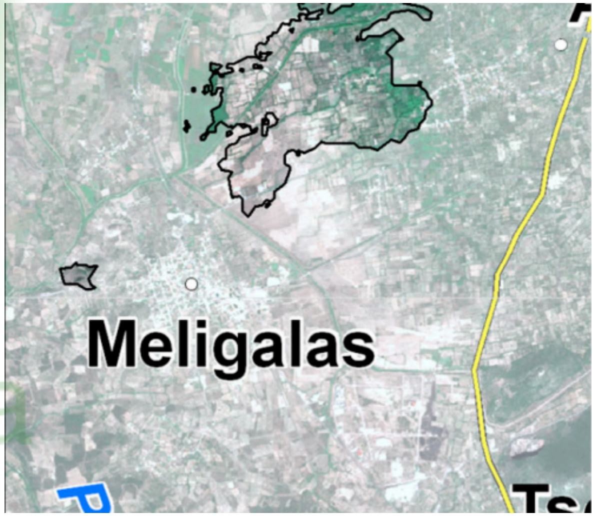

Peloponnese Peninsula, Gree

TerraSAR X   HH

Unsupervised Algorithm

Object layers computed from HH backscattering intensity image

↓

1) Automatic Segmentation

↓

2) Shape and Textural Features calculation and optimization

↓

3) SOM Classification

TexSOM Scheme

BACKSCATTER

HH

OBJECTS

Asymmetry

Lenght_on_Width

Mean

Shape_index

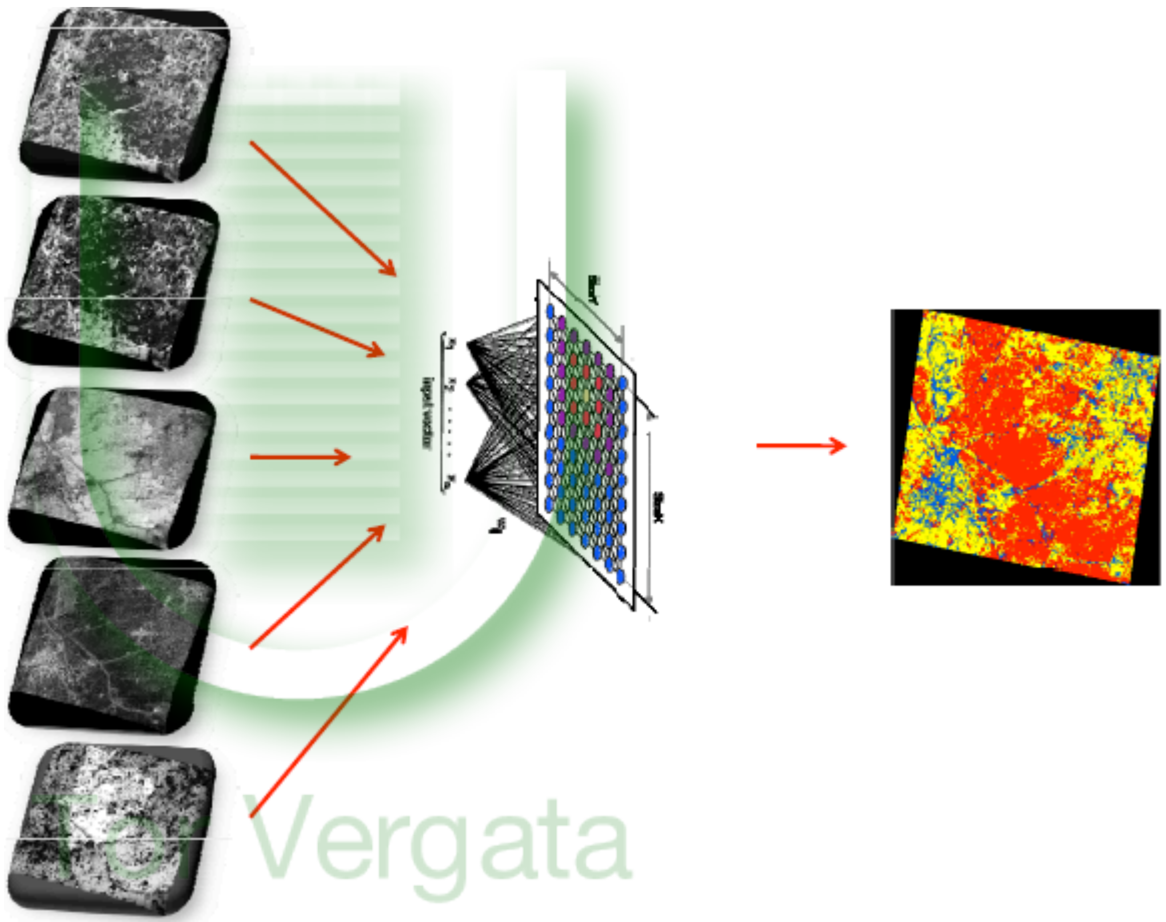

Classification result

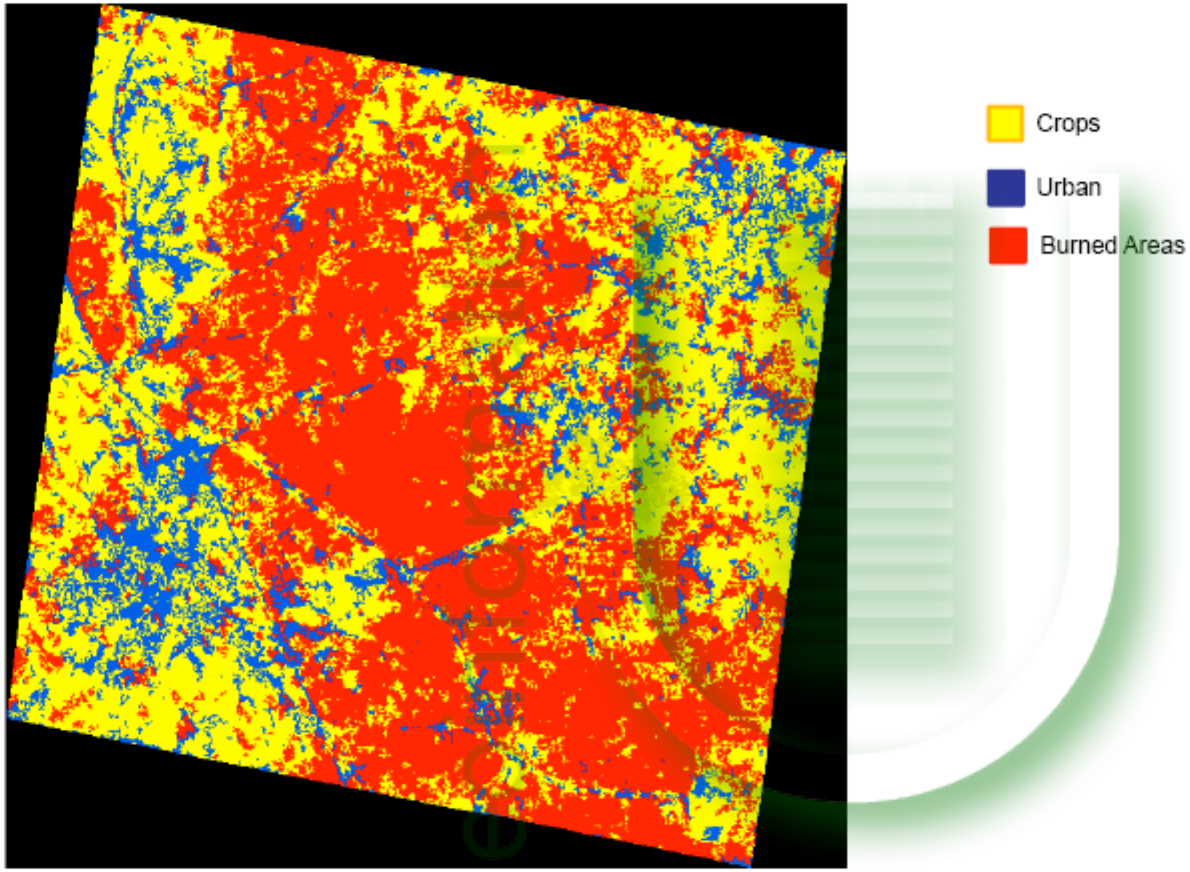

NO POST-CLASSIFICATION FILTER!!

Urban areas and streets are CRITICAL for firefighting

AUTOMATIC RETRIEVAL OF TECTONIC PARAMETERS WITH NEURAL NETWORKS AND SAR INTERFEROMETRY

The retrieval scheme

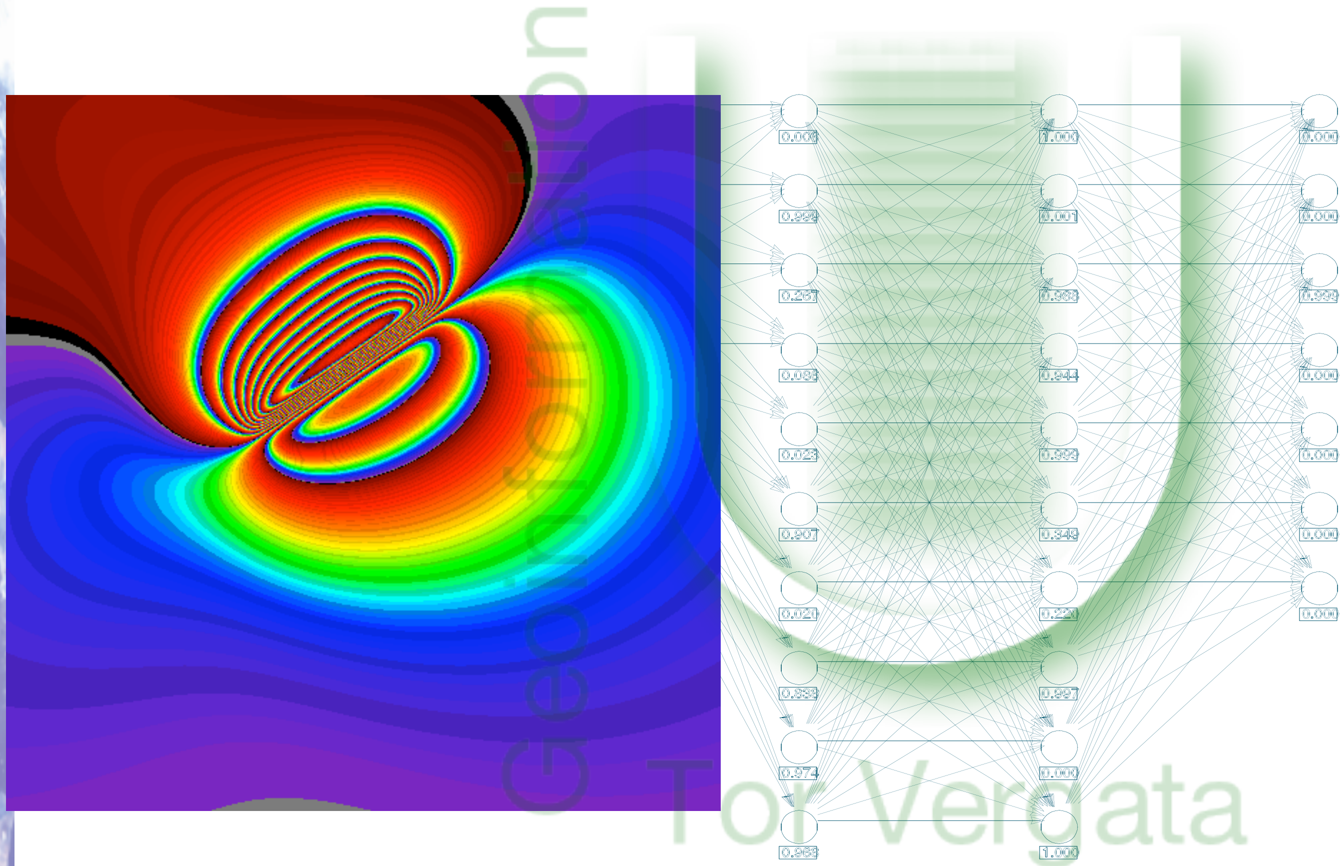

Fault dip
Fault strike
Width
Length
Slip*x*
Slip*y*
Slip*z*

TRAINING PHASE

Library of synthetic interferograms

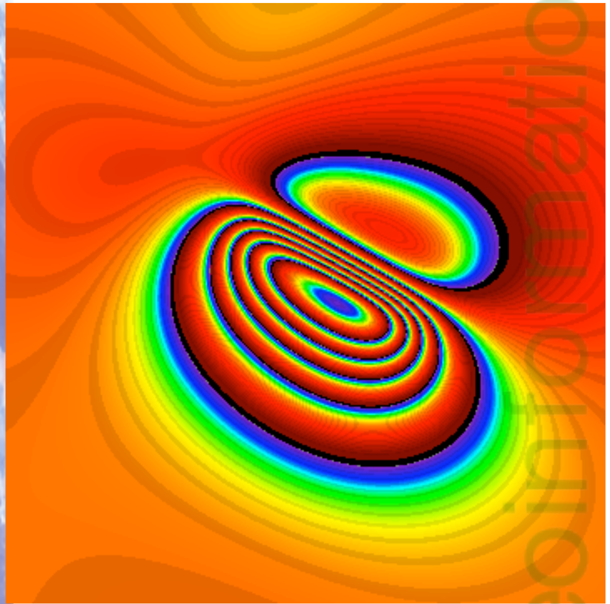

Normal fault

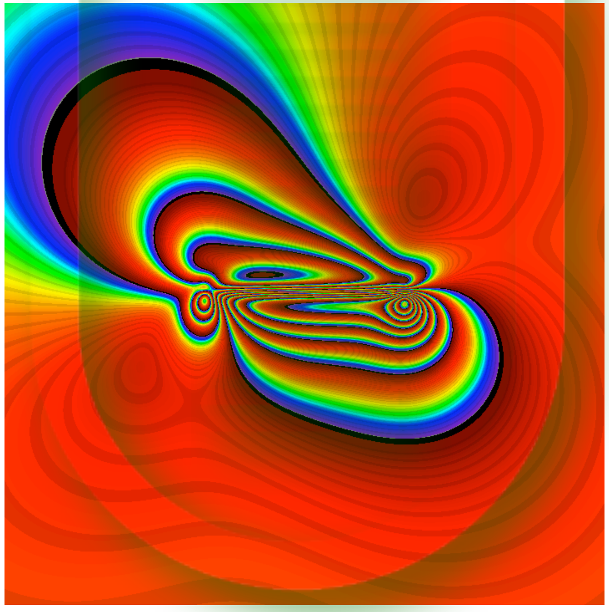

Strike slip fault

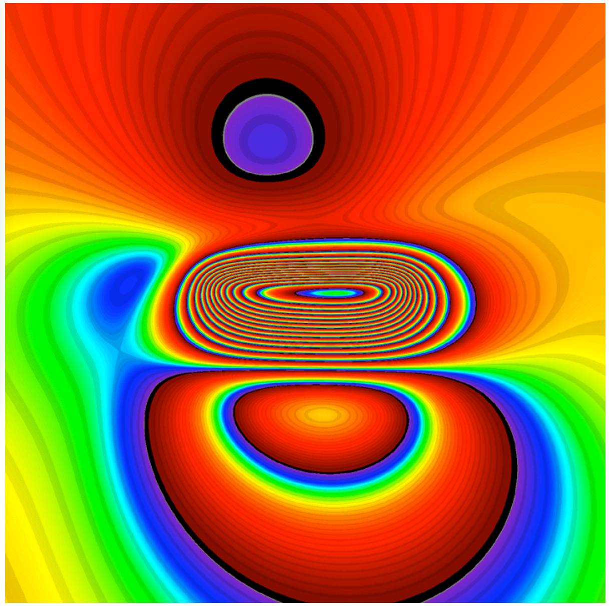

Thrust (reverse) faul

1200 interferograms generated

The neural architecture

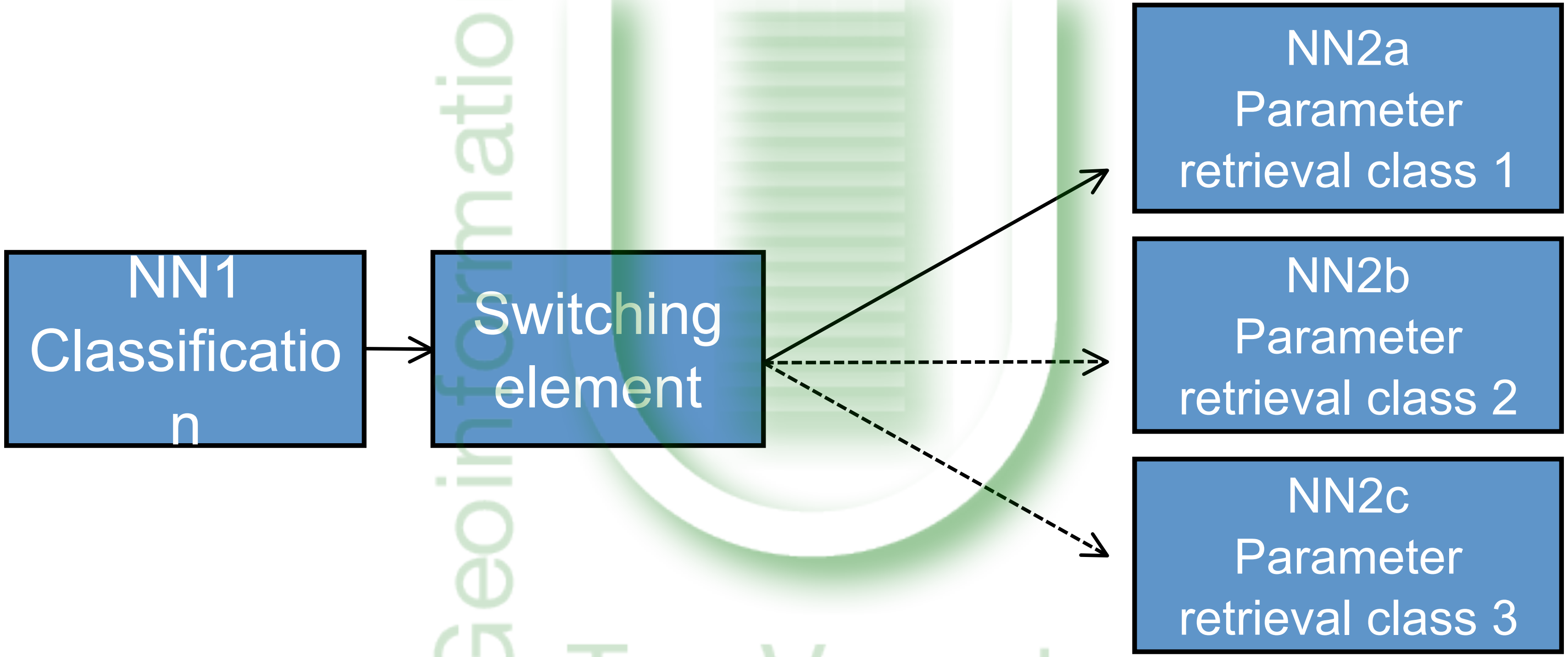

Experimental data

Colfiorito 1997: normal

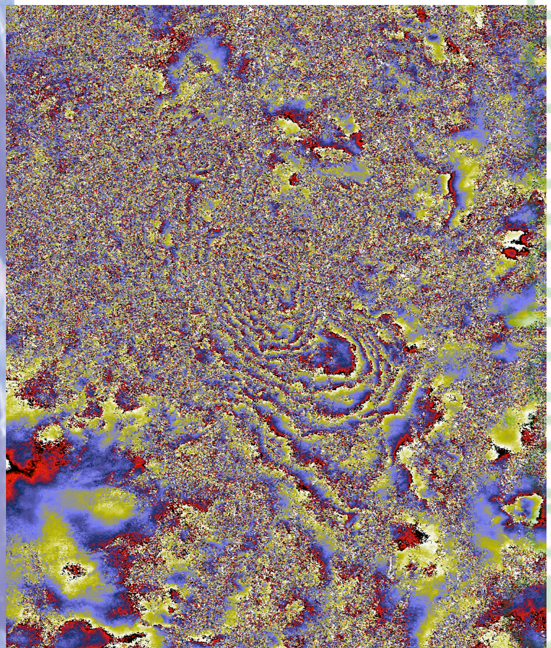

Bam 2003: Strike slip

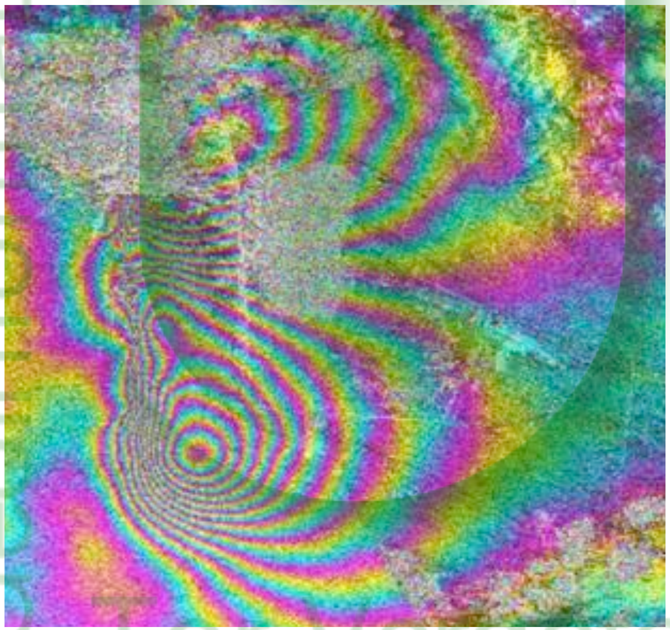

Northridge 1994: Revers

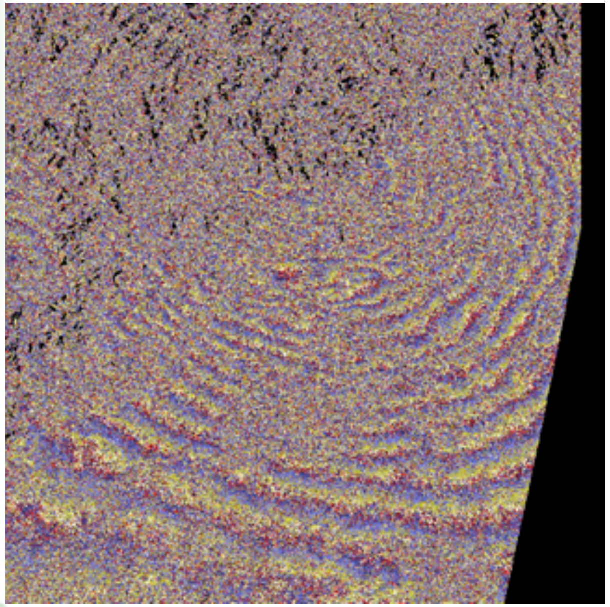

Our automatic results

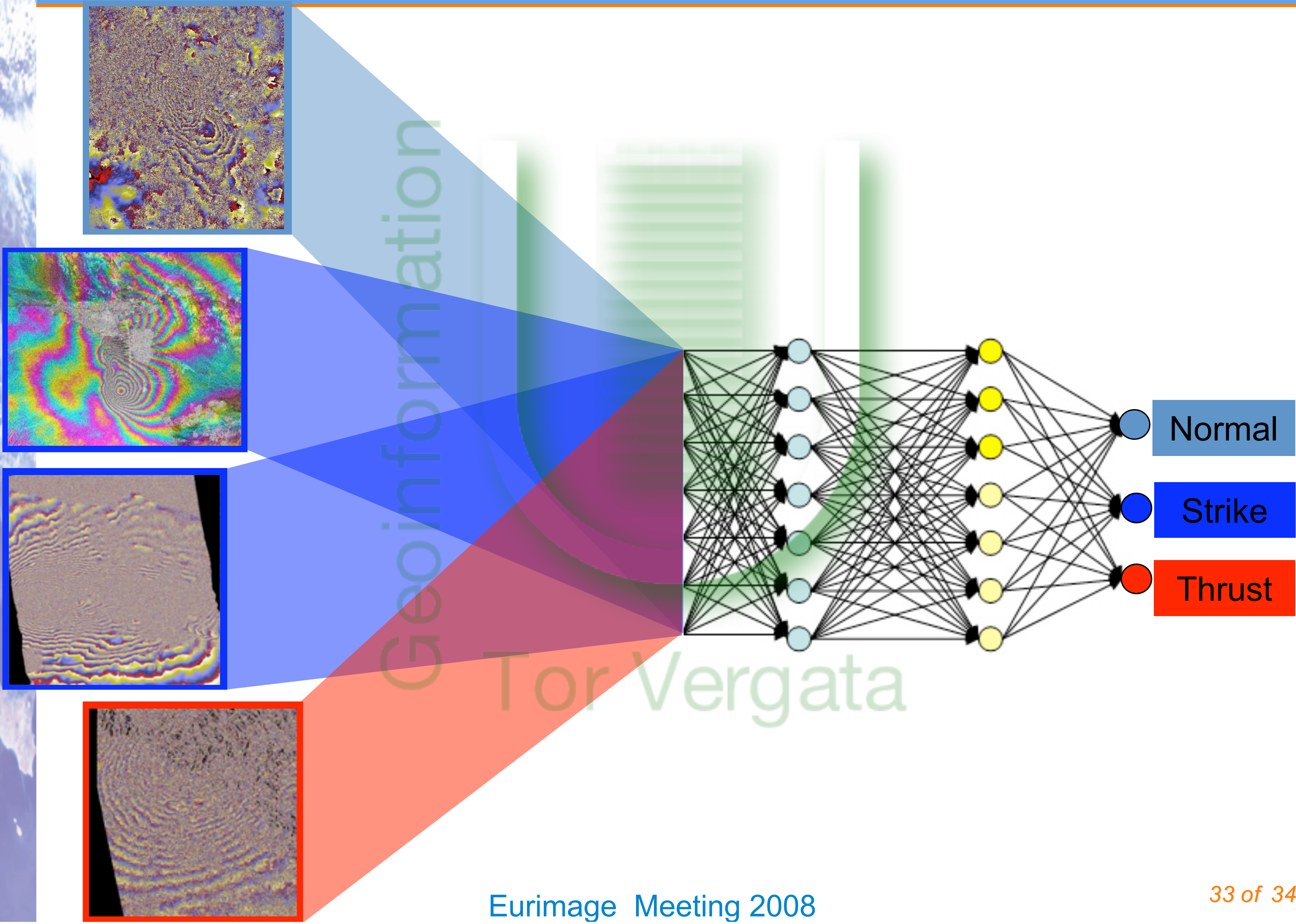

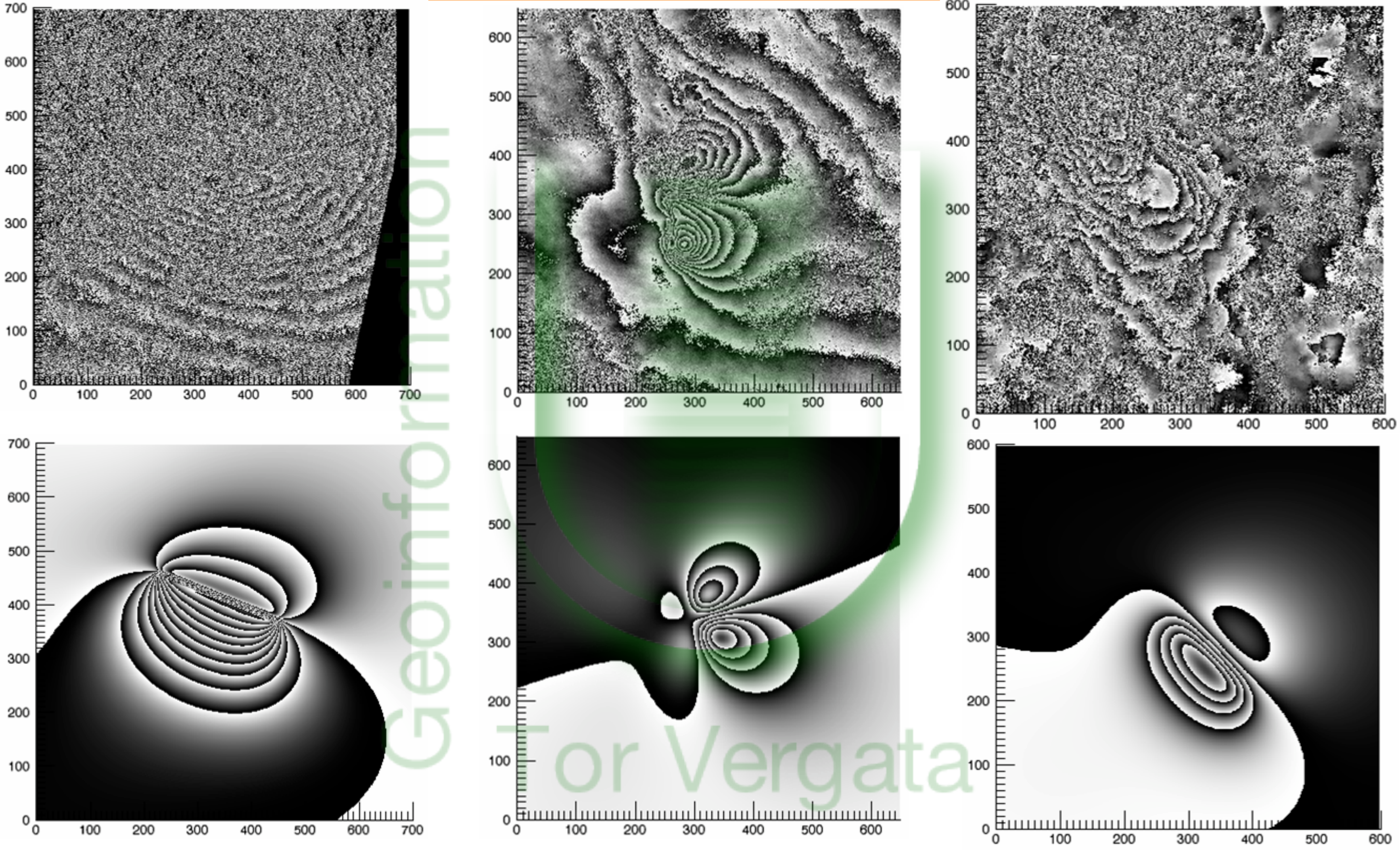

The analysis of surface deformation patterns could be extended to the interseismic displacements by using InSAR time series